Published in final edited form as:
Angew Chem Int Ed Engl. 2018 May 22; 57(21): 6230–6235. doi:10.1002/anie.201802509.

Localizing Antifungal Drugs to the Correct Organelle Can Markedly Enhance their Efficacy

Raphael I. Benhamou
School of Chemistry, Raymond&Beverly Sackler Faculty of Exact Sciences, Tel Aviv Universit, Tel Aviv, 6997801 (Israel)

Maayan Bibi, **Prof. Judith Berman**
Dept. of Molecular Microbiology & Biotechnology, George S. Wise Faculty of Life Sciences, Tel Aviv University, Tel Aviv, 6997801 (Israel)

Prof. Micha Fridman*
School of Chemistry, Raymond&Beverly Sackler Faculty of Exact Sciences, Tel Aviv Universit, Tel Aviv, 6997801 (Israel)

Abstract

A critical aspect of drug design is optimal target inhibition by specifically delivering the drug molecule not only to the target tissue or cell but also to its therapeutically active site within the cell. This study demonstrates, as a proof of principle, that drug efficacy can be increased considerably by a structural modification that targets it to the relevant organelle. Specifically, by varying the fluorescent dye segment an antifungal azole was directed from the fungal cell mitochondria to the endoplasmic reticulum (ER), the organelle that harbors the drug target. The ER-localized azole displayed up to two orders of magnitude improved antifungal activity and also dramatically reduced the growth of drug-tolerant fungal subpopulations in a panel of Candida species, which are the most prevalent causes of serious human fungal infections. The principle underlying the “target organelle localization” approach provides a new paradigm to improve drug potency and replenish the limited pipeline of antifungal drugs.

Keywords

antifungal agents; azole drugs; *Candida*; fluorogenic probes; organelle-targeting drugs

*T*o achieve the desired therapeutic response, an effective concentration of a drug must reach the infected organ or tissue and then engage its target within the pathogen cell. To date, drug delivery research has focused primarily on enhancing drug absorption and on trafficking it to specific sites of infection within organs and tissues.[1, 2] However, in eukaryotic pathogens, target proteins may be sequestered in membrane-bound organelles to which the drug has limited access.[3, 4] Directing the drug to localize to the relevant organelle within the

* mfridman@post.tau.ac.il.

Conflict of interest
The authors declare no conflict of interest.

Europe PMC Funders Author Manuscripts

pathogen by altering its chemical structure and properties has the potential to increase its pharmacological activity. Accordingly, improving the ability of a small molecule to localize to the specific organelle or domain that harbors its target can significantly improve its efficacy due to an increase in the local concentration of the inhibitor.[5–9]

Life-threatening fungal infections are associated with patients suffering from a compromised immune system; that is, patients with HIV/AIDS, cancer patients undergoing chemotherapy, or patients treated with immunosuppressants to prevent the rejection of organ transplants.[10] The evolutionary similarity between fungal and human eukaryotic cells limits the repertoire of antifungal drugs to only three major classes in wide clinical use: the polyenes, echinocandins, and azoles.[11, 12] The azole class of antifungal drugs, and in particular fluconazole (FLC, Figure 1), have been used widely and commonly to treat fungal infections because of their oral bioavailability, accessibility, and low cost, making them the first-line treatment for a broad spectrum of fungal infections.[12–14] Notably, FLC is the major antifungal drug available in many developing countries.[15]

Azole antifungals inhibit the cytochrome P-450-dependent lanosterol demethylase, also referred to as 14α-sterol demethylase (cytochrome P-450$_{DM}$), which is an essential enzyme in the biosynthesis of ergosterol, a major sterol component of the fungal plasma membrane.[16, 17] An analogous heme-containing enzyme catalyzes cholesterol biosynthesis in mammals. The efficacy of antifungal azoles is attributed to higher affinity for the fungal than for the mammalian cytochrome P-450$_{DM}$ at therapeutic concentrations.[18] Azole exposure causes the depletion of ergosterol and the accumulation of 14α-methylated sterols, thereby altering the structure of the fungal plasma membrane and consequently perturbing nutrient transport, chitin synthesis, and other cellular processes.[19–21]

Ergosterol biosynthesis is thought to take place primarily in the endoplasmic reticulum (ER), a membrane-bound organelle continuous with the nuclear envelope, in which most enzymes of ergosterol biosynthesis are localized.[22,23] Erg11p (the cytochrome P-450$_{DM}$ protein) localizes primarily to the fungal ER, and to a lesser degree to the cytoplasm and granular sites.[24] To establish the subcellular localization of antifungal azoles within fungal cells, we recently designed, synthesized and visualized two fluorescent antifungal azole probes, using fluorescent dyes attached to the pharmacophore of FLC (colored red, Figure 1), to produce antifungal azole probes **1** and **2**, respectively.

Surprisingly, both fluorescent azoles **1** and **2** primarily localized to, and accumulated in, the fungal mitochondria during the first hours of drug exposure.[25] Nonetheless, the activity of both probes required the presence of *ERG11*, the gene encoding the cytochrome P-450$_{DM}$, indicating that this enzyme is the target of these fluorescent probes.

In light of these results, we posited that localization of antifungal azoles in the wrong organelle could prevent much of the drug from reaching its target, thereby reducing drug efficacy and potentially leading to undesired side-effects due to off-target interactions. Thus, we set out to alter intracellular distribution of antifungal azoles and develop analogs that would localize primarily to the ER so as to enhance the concentration of the drug within the organelle that harbors its target.

The design of ER-directed antifungal azoles was based on a search for defined molecular motifs in small molecules known to localize to the ER. Included in the design was a fluorescent dye that enabled facile determination of the subcellular distribution of the resultant antifungal azole. While the guidelines for rational design of ER-directing molecular motifs remain obscure, structural analysis of fluorescent dyes that are commonly used for cell imaging revealed that ER-localized molecules were amphipathic and lipophilic with moderate-sized conjugated double bond systems.[26] For example, ER-membrane fluidity was recently studied by amphipathic and lipophilic sensors in which a BODIPY dye was attached to an aminocoumarin moiety and a membrane-anchoring aliphatic chain.[27] Accordingly, we designed and synthesized antifungal azole **3** (Figure 1) by attaching a 7-(diethyl)-aminocoumarin fluorescent dye to the azole pharmacophore (for synthetic procedures see the Supporting Information, Section 3, Scheme S1).

As negative controls for the antifungal activity tests, we synthesized azoles **4** and **5** (Figure 1). In these fluorescent azoles, the 1,2,4-triazole ring, which is predicted to interact with the iron atom in the heme core of cytochrome P-450$_{DM}$, was replaced by a 1,2,3-triazole ring that is predicted to form weaker interactions with the core heme iron and therefore to be a poor inhibitor of the enzyme. Based on density functional theory (DFT) calculations, the electron density on N-4 of the 1,2,4-triazole-based azole **3** (Figure 2 A) is 33% higher than that of the N-3 of the corresponding 1,2,3-triazole-based azole **5** (Figure 2 B). Docking computations suggested that FLC and both enantiomers of azoles **2**–**5** can bind within the catalytic domain of cytochrome P-450$_{DM}$ (Figure 2 C; Supporting Information, Section 5).

The antifungal activity of the 1,2,4-triazole-based azoles **2** and **3** was compared to that of the corresponding 1,2,3-triazole-based azoles **4** and **5** and to FLC by the broth double dilution method[28] using a panel composed of five different *Candida* species (Strains A–K, Table 1). Notably, the antifungal activity of azole **3** was improved significantly relative to both FLC and to the azole **2** in all of the species. The minimal inhibitory concentration (MIC) values of azole **3** were 4–64 fold and 16–256 fold lower than those of FLC and of azole **2**, respectively, against the entire tested panel of *Candida* strains.

The free fluorescent dyes dansyl acid and 7-(diethyl)-aminocoumarin 3-carboxylic acid had no detectable antifungal activity (MIC > 64 μg mL^{-1}). Furthermore, as expected, both 1,2,3-triazole-based azoles **4** and **5** had no antifungal activity against the tested *Candida* strains.

The fungistatic nature of azoles toward *Candida* imposes strong selection for the emergence of drug tolerance as well as drug resistance.[11, 29] Given the key role of azoles in the limited armamentarium of anti-*Candida* drugs, and that drug tolerance may be associated with increased persistence of infections,[30] the development of azoles that reduce tolerance is a highly desirable pharmacological property. To ask if the efficacy of azole **3** has any role in preventing the appearance of drug-tolerant subpopulations over time, we evaluated residual fungal cell growth after 48 and 72 hours by measuring the average cell density (OD_{600}) in broth microdilution assays at drug concentrations above the MIC (supra-MIC). Notably, MIC values were determined after 24 hours of incubation according to CSLI (Clinical and Laboratory Standards Institute) recommendations.[31] The cells treated with FLC or the dansyl-based azole **2** showed evidence of drug tolerance, as they continued to grow, albeit

slowly, at drug concentrations beyond the MIC determined at 24 h (arrows, Figure 3 A). Importantly, at supra-MIC drug concentrations, growth was significantly reduced for azole **3** relative to FLC and azole **2** measured at both 48 and 72 hours of incubation (Figure 3 B and C, respectively). Thus, azole **3** significantly reduces the degree of growth at supra-MIC, which reflects drug tolerant subpopulations that can be associated with FLC-persistent and recurrent infections.[32]

Subsequently, we compared the viability of mammalian cells exposed to azoles **2** and **3** or to FLC using both the human embryonic kidney cell line HEK 293 as well as primary human skin fibroblasts cells, which more closely mimic the physiological state of cells in vivo. Like FLC and azole **2**,[25] azole **3** did not significantly affect the viability of the tested mammalian cells ($IC_{50} \gg 25\ \mu g\ mL^{-1}$; for data see the Supporting Information, Section 7C, Figures S1 and S2) even at the maximal concentration tested (25 $\mu g\ mL^{-1}$), which was two to three orders of magnitude above the MIC range of azole **3** (Table 1).

To study if azole **3**, like FLC, acts by inhibiting cytochrome $P\text{-}450_{DM}$ or by a different or additional mode of action, we tested if growth inhibition requires the presence of the *ERG11* gene. *ERG11* encodes the cytochrome $P\text{-}450_{DM}$ target of azole drugs and is essential for aerobic growth unless *ERG3*, which encodes a C-5 sterol desaturase, is inactive. Thus, to test the requirement for the cytochrome $P\text{-}450_{DM}$ target, we used the *erg11*ΔΔ/*erg3*ΔΔ mutant strain, which is viable despite lacking the azole target cytochrome $P\text{-}450_{DM}$ and the C5 sterol desaturase. As a control, we used the parental strain (*C. albicans* SN152) from which the mutant was derived.[33] We compared the activities of FLC with azoles **2** and **3** against these two strains using the disk-diffusion assay method (Figure 4).

Importantly, growth of the *erg11*ΔΔ/*erg3*ΔΔ mutant was not sensitive to any of the azoles, including azole **3** (Figure 4 D–F, respectively). This also implies that the significant increase in antifungal activity of azole **3** relative to the other compounds is not due to the inhibition of other fungal targets. Rather, azole **3** appears to target cytochrome $P\text{-}450_{DM}$ more effectively, thereby dramatically reducing MIC as well as the growth of tolerant cells.

Subsequently, the subcellular distribution of azoles 2–5 was imaged by fluorescence microscopy of *C. albicans* SC5314 cells (Strain A, Table 1) for 120 minutes of drug exposure at 30 °C. In agreement with our previous work, dansyl-derived azole **2** localized to mitochondria (Figure 5 B), with a distribution pattern similar to that of the mitochondrion-specific dye MitoTracker Green FM (Figure 5 D). Importantly, the aminocoumarin-derived azole **3** exhibited a distinctive distribution with an apparent perinuclear ring decorated with associated membrane “flares” (Figure 5 F). This distribution pattern resembles that of the fungal ER-specific dye DiOC6 (Figure 5 H).[34] Co-localization of 3,3’-dihexyloxacarbocyanine iodide (DiOC6) and the diethyl aminocoumarin unit of azole **3** could not be distinguished as their excitation/emission spectra overlap. Thus, we compared the localization of azole **3** with that of Eno1-mCherry, a protein that localizes largely to the nucleus.[35] As expected of an ER localization pattern, which is continuous with the nuclear membrane, a fluorescent ring of azole **3** surrounded the Eno1-mCherry labeled nucleus (Figure 5 L). Thus, the localization of azole **3** is consistent with it being directed to the ER, unlike azole **2** that localizes to the mitochondria.

We analyzed the subcellular distribution of azole **3** in two additional *C. albicans* strains (C and F, Table 1). A similar ER-labeling pattern was observed, indicating that the subcellular distribution of antifungal azole **3** is not strain specific (Supporting Information, Section 7G, Figure S4). Notably, the 1,2,3-triazole-based **4** and **5** that were inactive against the tested *Candida* panel, displayed the same mitochondrial and ER-subcellular distribution as did their corresponding 1,2,4-triazole based azole **2** and azole **3**, respectively, indicating that the intracellular distribution of these azoles is not directly associated with their azole pharmacophore, nor with their antifungal activity (Supporting Information, Section 7G, Figure S5). Thus, the aminocoumarin-based azole **3** localized mainly to the ER, while the dansyl-based azole **2** localized mainly to the fungal mitochondria. Since cytochrome P-450$_{DM}$ localizes to the fungal ER, we propose that the improved activity of azole **3** relative to azole **2** may result from the increased concentration of this azole in the ER, which then leads to improved inhibition of the target enzyme that is primarily ER-localized.

In summary, we demonstrated that altering the subcellular distribution can improve the therapeutic properties of antifungal azoles that are often used as the first line of antifungal infection therapy. Antifungal azole **3** localized to the ER, which harbors the target of the azole class of antifungals, the cytochrome P-450$_{DM}$. The antifungal activity of azole **3** was 4–64-fold and 16–256-fold more potent than those of FLC and of azole **2**, respectively, against the entire tested panel of *Candida* strains. Moreover, unlike FLC and the mitochondria-directed azole **2**, ER-directed azole **3** significantly reduced drug tolerance, which can be associated with clinically persistent *C. albicans* infections. Furthermore, the antifungal activities of FLC, as well as azoles **2** and **3** were dependent on the presence of the target cytochrome P-450$_{DM}$. Taken together, this implies that the improved antifungal activity of aminocoumarin-based azole **3** may result from the higher local concentration of this azole in proximity to the ER-localized target enzyme. The results presented here suggest that the design of the ER-directed antifungal azoles has the potential to markedly improve the potency of these antifungals and to combat the rapid emergence of drug resistance.

Supplementary Material

Refer to Web version on PubMed Central for supplementary material.

Acknowledgements

We thank H. Engel and E. Pichinuk from the Blavatnik center for drug discovery for docking computations and cell viability experiments. We thank D. Sanglard, R. Ben Ami, C. Fairhead, B. Vincent, J. Usher, D. Soll, and S. Lindquist for providing *Candida* strains. We thank A. Rosenberg for help with technical aspects of the tolerance assays. This work was supported by the Israel Science Foundation Grant 314/13 (J.B.), by the European Research Council Advanced Award, 340087, RAPLODAPT (J.B.), and by Israel Science Foundation Grant 6/14 (Micha Fridman).

References

[1]. Tibbitt MW, Dahlman JE, Langer R. J Am Chem Soc. 2016; 138:704–717. [PubMed: 26741786]

[2]. Farokhzad OC, Langer R. ACS Nano. 2009; 3:16–20. [PubMed: 19206243]

[3]. Rajendran L, Knölker HJ, Simons K. Nat Rev Drug Discovery. 2010; 9:29–42. [PubMed: 20043027]

[4]. Sheff D. Adv Drug Delivery Rev. 2004; 56:927–930.

[5]. Huber KVM. Nat Chem Biol. 2017; 13:133–134. [PubMed: 28103226]
[6]. Mateus A, Gordon LJ, Wayne GJ, Almqvist H, Axelsson H, Seashore-Ludlow B, Treyer A, Matsson P, Lundbäck T, West A, et al. Proc Natl Acad Sci USA. 2017; 114:6231–6239.
[7]. Dubach JM, Kim E, Yang K, Cuccarese M, Giedt RJ, Meimetis LG, Vinegoni C, Weissleder R. Nat Chem Biol. 2017; 13:168–173. [PubMed: 27918558]
[8]. Zheng N, Tsai HN, Zhang X, Rosania GR. Mol Pharm. 2011; 8:1619–1628. [PubMed: 21805990]
[9]. Ding S, Qiao X, Suryadi J, Marrs GS, Kucera GL, Bierbach U. Angew Chem Int Ed. 2013; 52:3350–3354.Angew Chem. 2013; 125:3434–3438.
[10]. Brown GD, Denning DW, Gow NAR, Levitz SM, Netea MG, White TC. Sci Transl Med. 2012; 4:1–10.
[11]. Shapiro RS, Robbins N, Cowen LE. MicroBiol Mol Biol Rev. 2011; 75:213–267. [PubMed: 21646428]
[12]. Odds FC, Brown AJP, Gow NAR. Trends Microbiol. 2003; 11:272–279. [PubMed: 12823944]
[13]. Como J, Dismukes WE. N Engl J Med. 1994; 330:263–272. [PubMed: 8272088]
[14]. Kneale M, Bartholomew JS, Davies E, Denning DW. J Antimicrob Chemother. 2016; 71:3599–3606. [PubMed: 27516477]
[15]. Martin MV. J Antimicrob Chemother. 1999; 44:429–437. [PubMed: 10588302]
[16]. Nes WD. Chem Rev. 2011; 111:6423–6451. [PubMed: 21902244]
[17]. Lepesheva GI, Waterman MR. Biochim Biophys Acta Gen Subj. 2007; 1770:467–477.
[18]. Sheehan DJ, Hitchcock Ca, Sibley CM. Clin Microbiol Rev. 1999; 12:40–79. [PubMed: 9880474]
[19]. Ji H, Zhang W, Zhou Y, Zhang M, Zhu J, Song Y, Lü J, Zhu J. J Med Chem. 2000; 43:2493–2505. [PubMed: 10891108]
[20]. Ghannoum LBR, Mahmoud A. Clin Microbiol Rev. 1999; 12:501–517. [PubMed: 10515900]
[21]. Sagatova AA, Keniya MV, Wilson RK, Monk BC, Tyndall JDA. Antimicrob Agents Chemother. 2015; 59:4982–4989. [PubMed: 26055382]
[22]. Huh W-K, Falvo JV, Gerke LC, Carroll AS, Howson RW, Weissman JS, O'Shea EK. Nature. 2003; 425:686–691. [PubMed: 14562095]
[23]. Breker M, Gymrek M, Moldavski O, Schuldiner M. Nucleic Acids Res. 2014; 42:726–730.
[24]. Shakoury-Elizeh M, Protchenko O, Berger A, Cox J, Gable K, Dunn TM, Prinz WA, Bard M, Philpott CC. J Biol Chem. 2010; 285:14823–14833. [PubMed: 20231268]
[25]. Benhamou RI, Bibi M, Steinbuch KB, Engel H, Levin M, Roichman Y, Berman J, Fridman M. ACS Chem Biol. 2017; 12:1769–1777. [PubMed: 28472585]
[26]. Xu W, Zeng Z, Jiang JH, Chang YT, Yuan L. Angew Chem Int Ed. 2016; 55:13658–13699.Angew Chem. 2016; 128:13858–13902.
[27]. Lee H, Yang Z, Wi Y, Kim TW, Verwilst P, Lee YH, Han GI, Kang C, Kim JS. Bioconjugate Chem Bioconjug Chem. 2015; 26:2474–2480.
[28]. Benhamou RI, Steinbuch KB, Fridman M. Chem Eur J. 2016; 22:11148–11151. [PubMed: 27258738]
[29]. Anderson JB. Nat Rev. 2005; 3:547–556.
[30]. Rosenberg A, Ene IV, Dahan AM, Segal ES, Colombo AL, Bennett Rj, Berman J. BioRxiv Prepr. 2017; doi: 10.1101/206359
[31]. Clinical and Laboratory Standards Institute. Reference Method for Broth Dilution Antifungal Susceptibility Testing of Yeasts; Approved Method M27-A3. 2002
[32]. Desai JV, Mitchell AP, Andes DR. Cold Spring Harbor Perspect Med Cold Spring Harb Perspect Med. 2014; 4:a019729.
[33]. Vincent BM, Lancaster AK, Scherz-Shouval R, Whitesell L, Lindquist S. PLoS Biol. 2013; 11:e1001692. [PubMed: 24204207]
[34]. Koning, aJ; Lum, PY; Williams, JM; Wright, R. Cell Motil Cytoskeleton. 1993; 25:111–128. [PubMed: 7686821]
[35]. Gerami-Nejad M, Dulmage K, Berman J. Yeast. 2009; 26:399–406. [PubMed: 19504625]

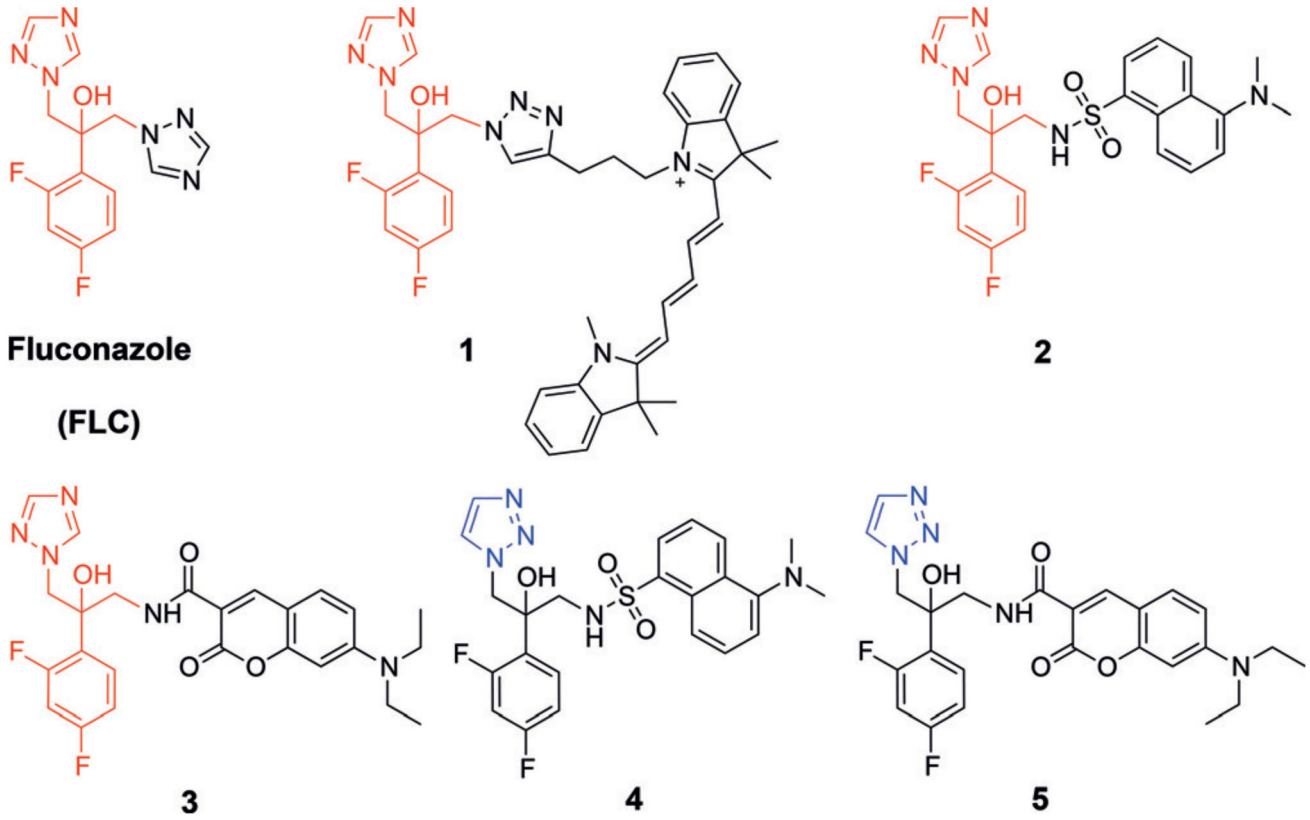

Figure 1.

Structures of FLC, inherently fluorescent antifungal azoles **1**–**3**, and azoles **4** and **5** (the 1,2,3-triazole derivatives of **2** and **3**, respectively). The pharmacophore of the antifungal azoles is colored red and the 1,2,3-triazole ring of **4** and **5** is colored blue.

Europe PMC Funders Author Manuscripts

Europe PMC Funders Author Manuscripts

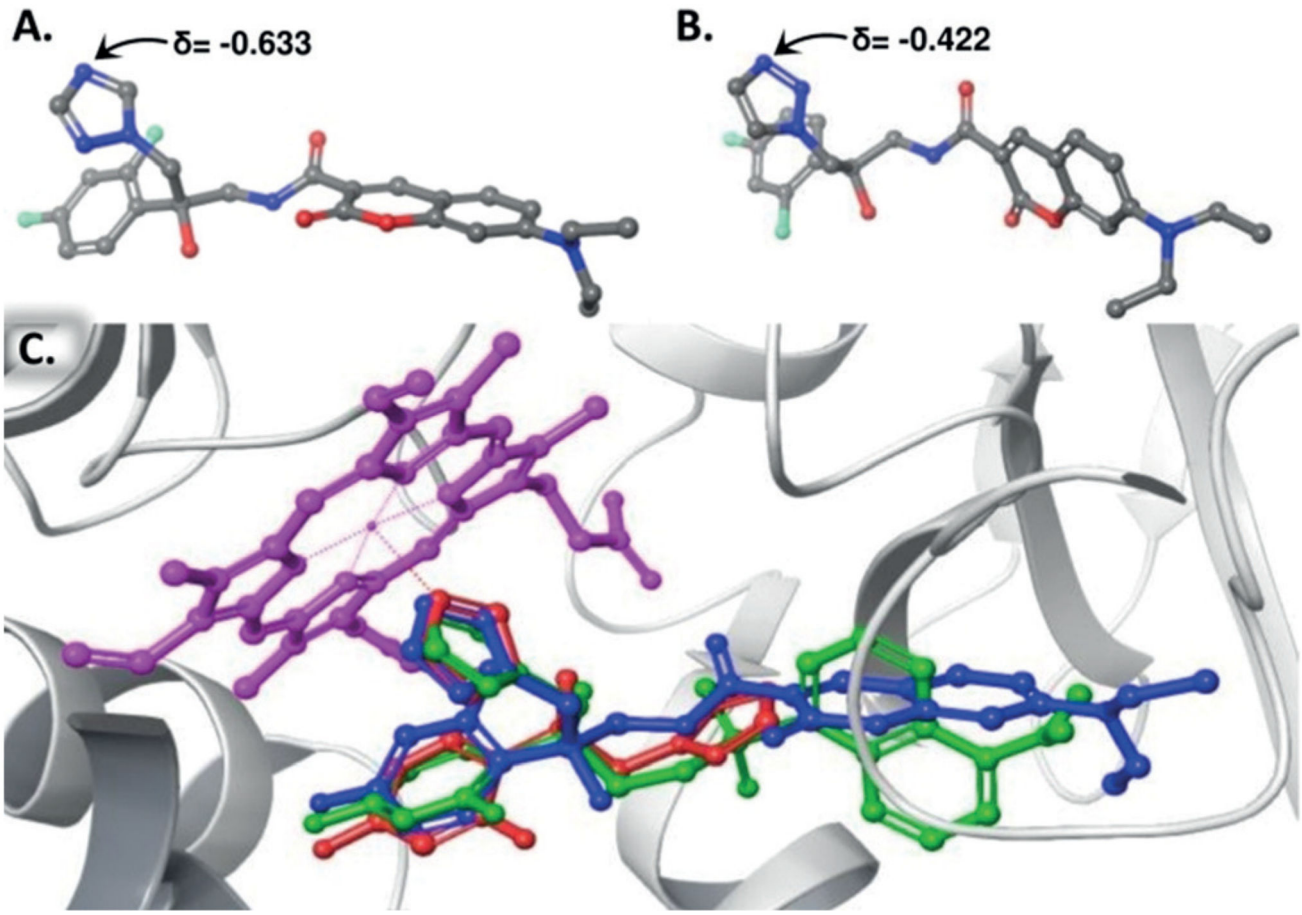

Figure 2.

A) Partial charge value of the N-4 of the 1,2,4-triazole-based **3**. B) Partial charge value of the N-3 of the 1,2,3-triazole-based **5**. The partial charges were assigned according to the OPLS3 force field calculations. C) Docked structure of the *R*-enantiomer of azole **2** (green), the *R*-enantiomer of azole **3** (blue), and FLC (red) on a crystal structure of *S. cerevisae* cytochrome $P450_{DM}$ (PDB ID: 4ZDY). Protein residues are shown as grey ribbons with the heme prosthetic group in magenta.

Europe PMC Funders Author Manuscripts

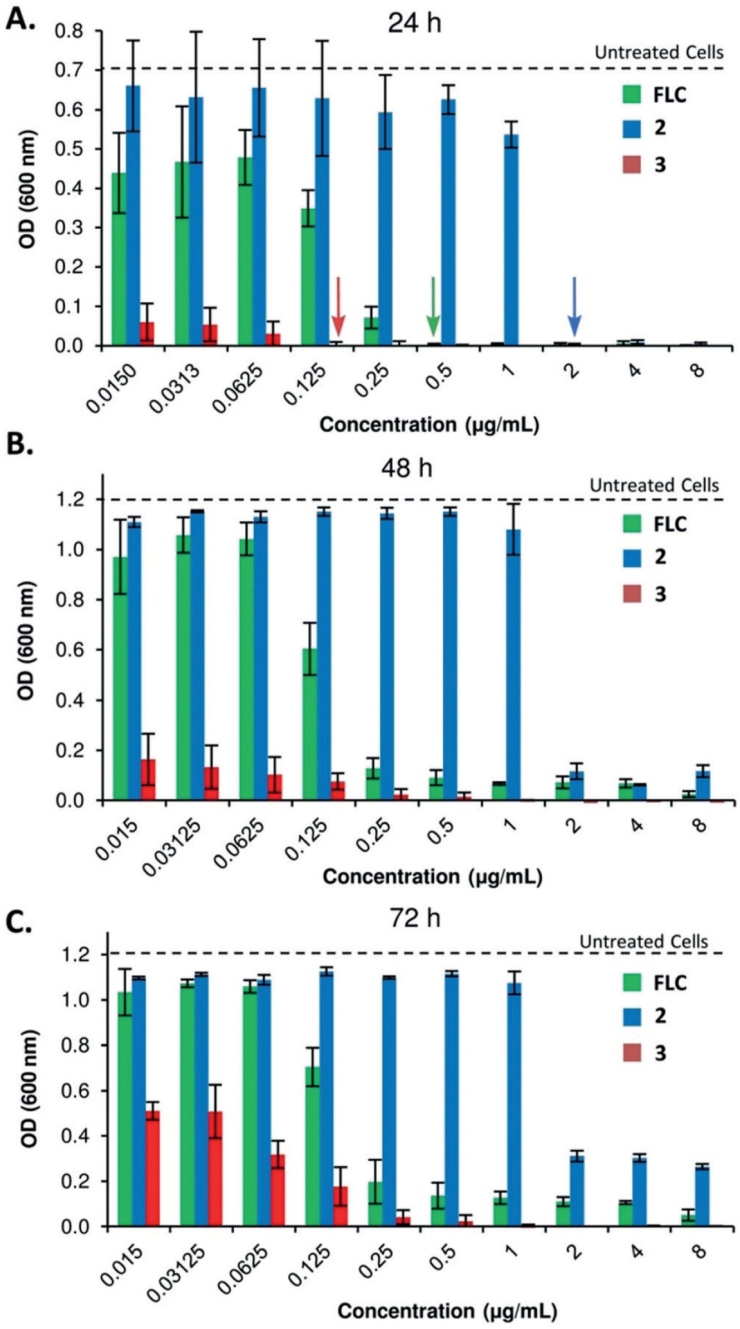

Figure 3.

Appearance of drug tolerant subpopulations over time in *C. albicans* SN152 at supra-MIC concentrations. A) Cell density after 24 hours (MIC is marked with an arrow). B) Cell density after 48 hours. C) Cell density after 72 hours.

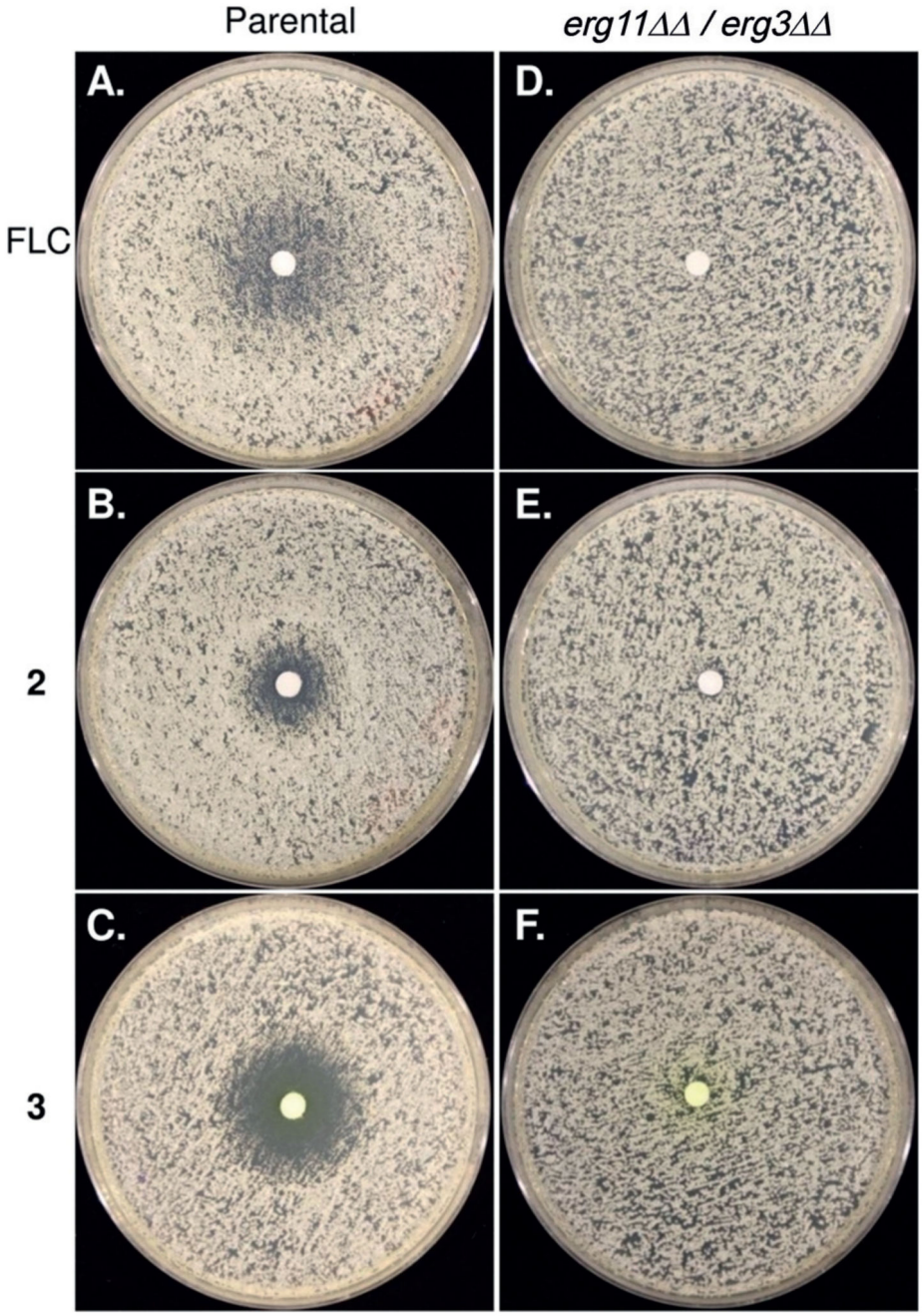

Figure 4.

Drug responses of *C. albicans* SN152 (parental) and ergosterol biosynthesis mutant strain (*erg11ΔΔ*/ *erg3ΔΔ*) by the disk diffusion assay. Cells were plated on casitone plates with disks containing 25 μg of the test compound placed in the center of the plates and were incubated for 24 hours at 30 °C.

Europe PMC Funders Author Manuscripts

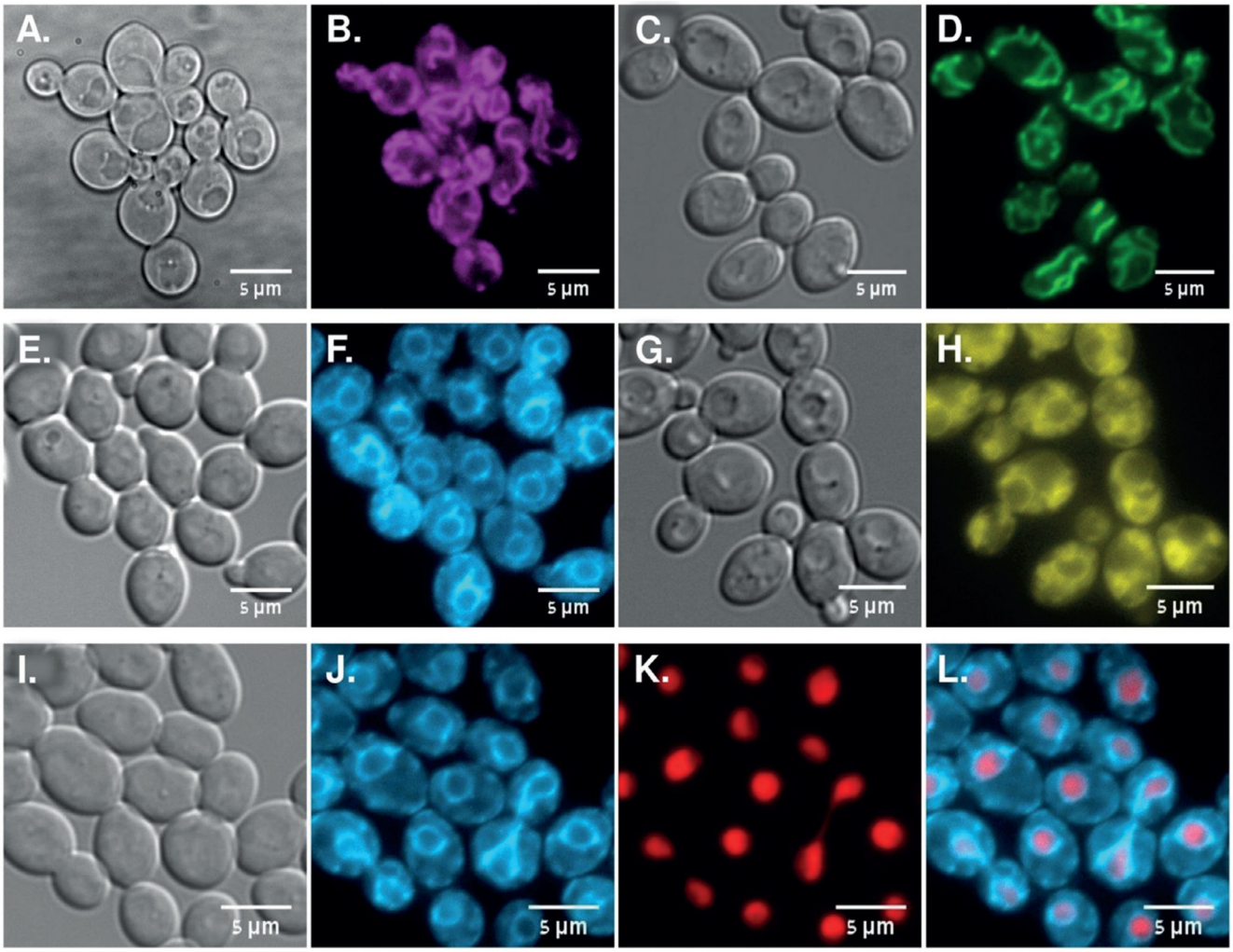

Figure 5.

Localization of antifungal azoles relative to mitochondrial, ER, and nuclear structures in live *C. albicans* SC5314 cells. A,B) Azole **2** (magenta, 10 μg mL^{-1}) after 120 min. C,D) MitoTracker (green, 10 nM) after 60 min. E,F) Azole **3** (cyan, 1 μg mL^{-1}) after 120 min. G,H) DiOC6—ER tracker (yellow,1 μg mL^{-1}) after 5 min. I,J,K,L) Azole **3** (cyan) in cells expressing Eno1-mCherry nuclear protein (red) after 120 min. The bandpass filters used to image azole **2** were excitation 390/40 nm and emission 520/20 nm and filter sets used to image **3** and DiOC6 staining were excitation 440 nm and emission 480/40 nm. For MitoTracker green FM excitation 470 nm and emission 525/50 nm and for Eno1-mCherry excitation 585 nm and emission 630/75 nm.

Europe PMC Funders Author Manuscripts

Table 1
Antifungal activities of FLC and the fluorescent azoles.

Compound MIC [μg/mL]					
Yeast strain	**FLC**	**2**	**3**	**4**	**5**
A. *C. albicans* SC5314	1	2	0.062	>64	>64
B. *C. albicans* 90028	0.5	2	0.007	>64	>64
C. *C. albicans* 24433	1	2	0.125	>64	>64
D. *C. albicans* P-87	0.5	2	0.007	>64	>64
E. *C. albicans* DSY3553	0.5	4	0.125	>64	>64
F. *C. albicans* SN152	0.5	2	0.125	>64	>64
G. *C. tropicalis* 660	0.5	2	0.007	>64	>64
H. *C. parapsilosis* 90018	0.5	2	0.031	>64	>64
I. *C. parapsilosis* 22019	1	8	0.125	>64	>64
J. *C. guilliermondii* B-3163	4	8	0.125	>64	>64
K. *C. dubliniensis* Wu284	0.25	0.5	0.062	>64	>64

All MICs were determined using the broth double-dilution method starting with 64 μg/mL of each compound.[28] Cells were grown in RPMI 1640 medium at 37° under 5% CO_2 for 24 h. Each concentration was tested in triplicate, and results were confirmed by two independent sets of experiments.